Morphology Development of High-Density Rigid Polyurethane Foam upon Compression by On-Line Scanning Electronic Microscope

Lei Shi,[1,2] Zhong-Ming Li[2]

[1]*College of Materials Science and Engineering, Southwest University of Science and Technology, Mianyang 621002, Sichuan, People's Republic of China*
[2]*State Key Laboratory of Polymer Materials Engineering, College of Polymer Science and Engineering, Sichuan University, Chengdu 610065, Sichuan, People's Republic of China*

Received 1 August 2006; accepted 4 March 2007
DOI 10.1002/app.26410
Published online 1 May 2007 in Wiley InterScience (www.interscience.wiley.com).

ABSTRACT: The high-density rigid polyurethane foam (RPUF) was obtained by airtight cast molding. The morphology development during the compressive fracture process of RPUF was observed on-line by a scanning electronic microscope (SEM). In the early stage of loading, the deformation of samples came from the tiny shape change in the cells' windows. As the load increases, some creases were formed in some cell windows in the vertical direction of loading, and the creases enlarged and resulted in the cracks across the whole cells. Moreover, during the deformation process, a failure band was formed in the weakest position. © 2007 Wiley Periodicals, Inc. J Appl Polym Sci 105: 2008–2011, 2007

Key words: high-density rigid polyurethane foam; microstructure; compressive fracture

INTRODUCTION

Polymeric foams are widely used in a variety of applications for the advantages of their energy absorption characteristics, thermal properties, and specific strength.[1,2] Especially, rigid polyurethane foam (RPUF) is playing an important role in many industries and contributing greatly to our daily lives, such as shipbuilding, footwear, construction, cars, insulation, furniture, car seating, and packaging.[3,4] Nowadays, primary attention is being paid to developing substitute of blowing agents[5] and improving mechanical properties of RPUF.[6,7] The deformation process and failure mechanism of RPUF are, however, rarely investigated, especially for high-density RPUF, though they are of particular significance for the foam's structure design and manufacture. In this work, the compressive deformation process of a high-density RPUF was observed on-line by a scanning electronic microscope (SEM). In addition, the stress–strain behavior of the RPUF was also chiefly discussed.

Correspondence to: Z. M. Li (zm_li@263.net.cn).
Contract grant sponsor: National Natural Science Foundation of China and Engineering Physical Academy of China; contract grant number: 10276024.
Contract grant sponsor: Program for Changjiang Scholars and Innovative Research Team in University (PCSIRT).

Journal of Applied Polymer Science, Vol. 105, 2008–2011 (2007)

EXPERIMENTAL

Materials

1. Polyether polyol, GR-4110G, made from polypropylene oxide and a sucrose/glycerin base, available from GaoQiao Petro (Shanghai, China). The manufacturer specifies the following properties: density (25°C), 1.1 g/cm^3; typical hydroxyl number, 430 mg KOH equiv/g of resin; viscosity (25°C), 3283 cps; functionality, 4.1; average molecular weight, 550 g/mol.
2. Silicone glycol copolymer, a surfactant.
3. Triethanolamine, a catalyst with a density of 1.122 g/cm^3 available from Shanghai Chemical Reagent (Shanghai, China).
4. Dibutyltin dilaurate, a catalyst with a density of 1.052 and a Sn content of 18% available from Sichuan Chemical Reagent (Chengdu, China).
5. Distilled water, blowing agent.
6. Polyisocyanate, N200, PAPI available from ChangFeng Chemical (ChongQing, China). The manufacturer specifies the following properties for N200: polyisocyanate equivalent weight, 126.5 g; —NCO content by weight, 30%; viscosity (25°C), 215 cps; functionality, 2.2.

Processing of foams

RPUF was prepared by cast molding, whose detailed description has been reported elsewhere.[2,8] Components, (1)–(5) in a certain weight ratio, were mixed

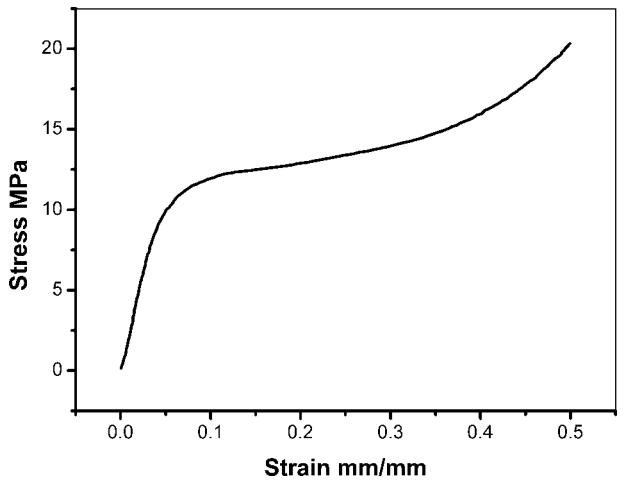

Figure 1 Typical stress–strain curve of RPUF.

and stirred together using an electric stirrer until a uniform mixture was obtained. The polyisocyanate (6) was then added, and the mixture is stirred for additional 30 s. The addition of the polyisocyanate initiates formation of the foam by reacting with the water to give CO_2. The mixture was finally poured quickly into a mold with a lid. The foam expanded to fill the entity until it was compressed by the lid. The foam obtained was postcured in an oven for 4 h at 100°C.

Compressive test

The foam with a density of 0.40 g/cm^3 was cut into $8 \times 8 \times 8$ mm^3 sheets for compressive test. The compressive test was performed under ambient conditions on a MTS880-50KN fatigue-testing machine using displacement-control pattern. The loading speed was 5 mm/min and the samples were compressed until fracture. The SEM images of the foam when compressed were taken at different displacements. To obtain the compressive stress–strain curve, the cylindrical sample was measured under ambient conditions with an AG-10TA universal electronic tensile machine (Shimadzu, Japan). The cylinders with 50 mm in diameter and 50 mm in length were machined from the rough foams whose skin was peeled. The speed of the crosshead was 2 mm/min.

RESULTS AND DISCUSSION

The typical compressive stress–strain curve for RPUF sample with a density of 0.40 g/cm^3 is shown in Figure 1. It apparently exhibits three different regions: initial linear loading (elastic), plateau (yielding), and final sharp rise in compressive stress (compact). In the elastic region, the RPUF specimen reveals an abrupt increase in stress as the strain increases. The modulus of foam can be obtained from this region. The initial linear elasticity is controlled by elastic axial compressive and bending of cell edges, stretching of cell faces, and compression of gas within the closed cells.[9] In the yield region, the compressive stress increases a little with the increase in strain. The cells collapse via buckling, plastic deformation, or rupture of cell walls and edges.[9] In the compact region, the compressive stress shows a sharp rise with increasing strain because of foam densification, which is associated with completely collapsed cells being compacted against each other and the stress rise steeply as the solid cell wall material is pressed together.[9]

Figure 2 reveals a representative foam structure of RPUF in the rise foam direction. The cell shape is approximately spheroidal, with a wide cell size distribution. Some studies[10] indicated that when the gas volume fraction exceeds 74%, dispersed spherical bubbles deform into multisided polyhedra. Usually, the cell structure of RPUF was, hence, a closed cellular polyhedron structure for low density foam[11,12] or approximate spheroid for high density foam.[2,8] However, some tiny cells exist in the cell wall, as shown in Figure 2. When the blowing reaction was close to end and the viscosity became very high, the pressure of the gas produced by the reaction between water and polyisocyanate was not strong enough to destroy the struts and entered the larger cells. Consequently, this gas formed these tiny cells in the larger cell windows. Besides, some cells' windows were destroyed during machining the sample, as shown in Figure 2.

The SEM micrographs exhibiting the overall morphology development process of RPUF samples upon compression are shown in Figure 3. At the

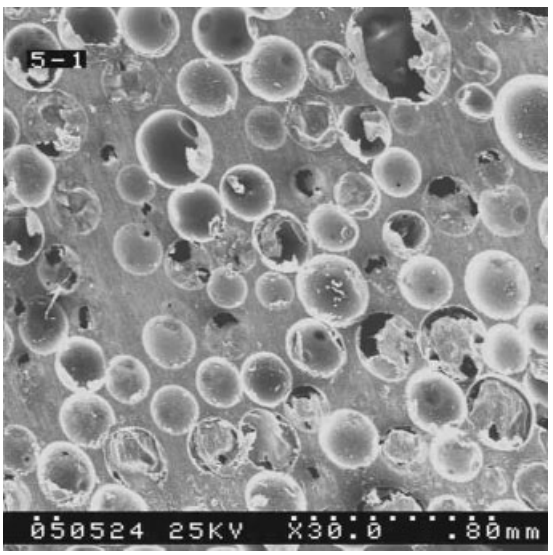

Figure 2 Representative SEM micrograph of RPUF.

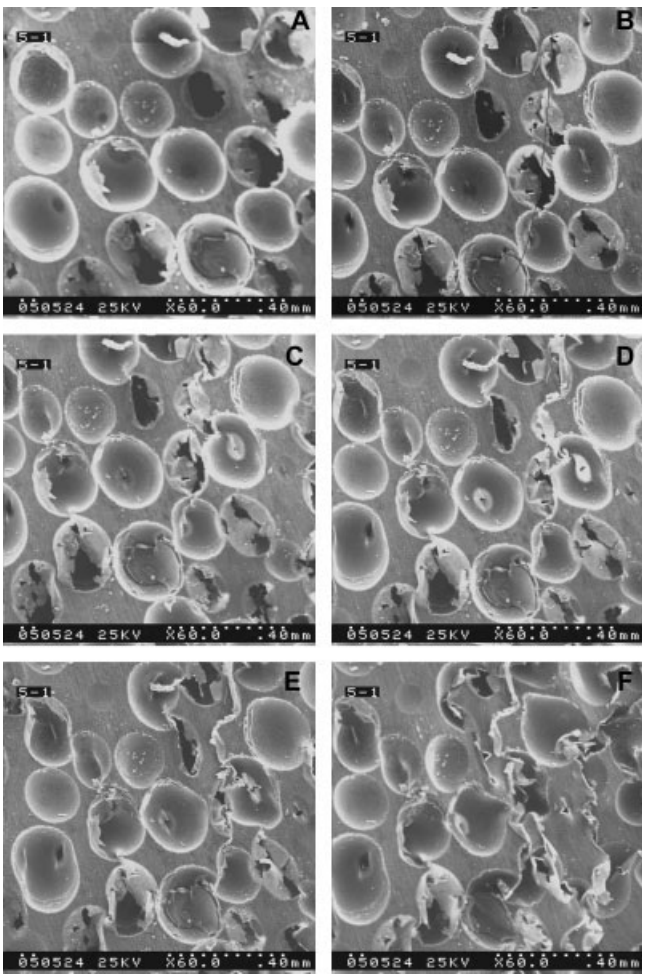

Figure 3 SEM micrographs of overall morphology development process of RPUF samples upon compression. Load: (a) 20, (b) 405, (c) 493, (d) 528, (e) 548, and (f) 569*N*.

early stage of loading, the cells generate minute elastic deformation and their shapes are changed to ellipsoid, as shown in Figure 3(a). This process corresponds to the elastic region of stress–strain curve. According to Figure 3(b), when the load gradually increases, the cracks begin to occur at the weakest points in the foam. The proceeding direction of the cracks is vertical to the loading direction, in which the obvious deformation of cells can be observed. As shown in Figure 3(c), when larger load is applied, the cells in the loading direction are deformed heavily, even broken, and subsequently, the struts between two broken cells are damaged. However, the cells in other directions almost remain unchanged except the minute deformation. This stage reflects the yield region of stress–strain curve. Finally, the foam collapses and is crushed in the direction of crack [Fig. 3(d–f)], which is related to the compact region of stress–strain curve.

The SEM micrographs revealing the fracture process of a single cell are shown in Figure 4. No crack in the surface of cell is observed at the beginning of

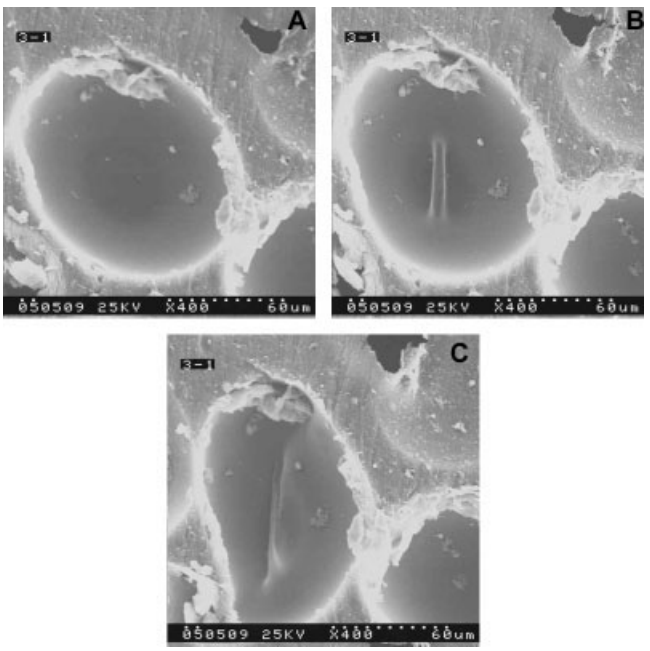

Figure 4 SEM micrographs for failure process of a single cell in the sample. Load (a) 58, (b) 523, (c) 837*N*.

loading [Fig. 4(a)]. The macroscopic deformation of the sample is due to accumulative tiny shape change generated in each cell windows. As the load increases, creases are formed in some cell windows in the vertical direction of loading [Fig. 4(b)]. When the load further increases, the creases enlarge and evolve into cracks across the whole cell, resulting in collapse of the cell at last [Fig. 4(c)].

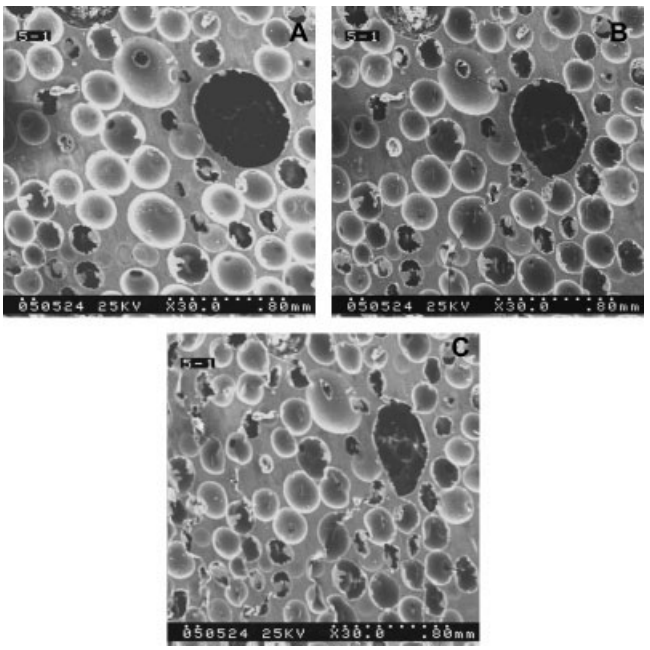

Figure 5 SEM micrographs for failure process of RPUF with weak points. Load (a) 19, (b) 405, and (c) 528*N*.

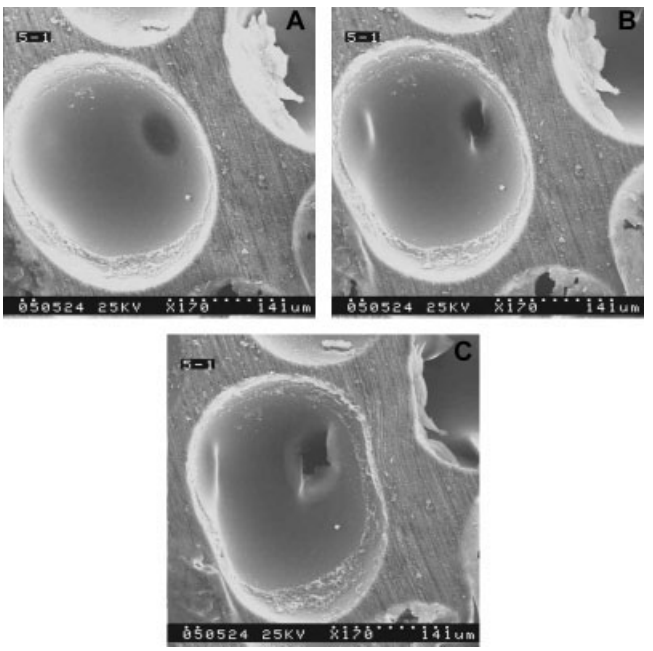

Figure 6 SEM micrographs for failure process of cell with innate flaw in RPUF. Load (a) 19, (b) 493, and (c) 568*N*.

Here arises a problem why many cells do not have obvious deformation when the foam collapses completely? This is probably due to the formation of crack band and the distortion of some cells with some innate flaws. The crack band vertical to the compressive direction is shown in Figure 3(b) (its position marked by the lines). Upon compression, the deformation first happens in the weakest positions of foam. If the weak positions are closed to each other, the deformed cells can connect to form a crack band. The cellular structure of the crack band is weaker than others. So when the load increases, the further deformation and breakdown first generate in the crack band while other cellular structure can remain tentatively until the cell system in crack band collapses completely. It is worth noting that the crack band in the sample is not certain to be vertical to the direction of load, because the distribution of weak positions in RPUF is dependent on the cell microstructure. Also, the weak positions in the RPUF can probably result in the crack band under shear stress, as shown in Figure 5 (the position marked by the lines). With increasing of the load, the cells on the shear crack band are damaged continuously. Finally, the cells collapse completely. Likewise, other cells can also tentatively remain their initial structure.

Figure 6 depicts the breakdown process of the cell with an initial flaw (the position marked by the lines). For the cells with such an initial flaw as minute bubbles or the creases in the wall of the cells will be the sources that induce cracks. Upon loading, first the cracks form in these locations.

CONCLUSIONS

In summary, the failure process of RPUF upon compression is related to its initial cellular structure. The early deformation mainly represented accumulative effect of tiny shape change generated in the cells' windows. As the load increases, creases are formed in some cell windows in the vertical direction of loading, and then evolved into cracks that caused fracture of the whole cell. Besides, during deformation, two types of crack bands are generated, which are formed due to compression or shear stress.

References

1. Goods, S. H.; Neuschwanger, C. L.; Whinnery, L. L.; Nix, W. D. J Appl Polym Sci 1999, 74, 2724.
2. Yin, B.; Li, Z. M.; Quan, H.; Zhou, Q. M.; Tian, C. R.; Yang, M. B. J Elastom Plast 2004, 36, 333.
3. Chang, L. C.; Xue, Y.; Hsieh, F. H. J Appl Polym Sci 2001, 81, 2027.
4. Shi, L.; Li, Z. M.; Xie, B. H.; Wang, J. H.; Tian, C. R.; Yang, M. B. Polym Int 2006, 55, 862.
5. Bogdan, M.; Williams, D.; Verbiest, P. J Cell Plast 2001, 37, 58.
6. Kim, D. S.; Macosko, C. W. Polym Eng Sci 2000, 40, 2205.
7. Petrovic, Z. S.; Javni, I.; Waddon, A.; Banhegyi, G. J Appl Polym Sci 2000, 76, 133.
8. Shi, L.; Li, Z. M.; Yang, M. B.; Yin, B.; Zhou, Q. M.; Wang, J. H. Polym Plast Technol Eng 2005, 44, 1323.
9. Tu, Z. H.; Shim, V. P. W.; Lim, C. T. Int J Solids Struct 2001, 38, 9267.
10. Mondal, P.; Khakhar, D. V. J Appl Polym Sci 2004, 93, 2821.
11. David, G. G.; Joseph, R. H.; Donald, E. H. J Cell Plast 1980, 16, 159.
12. Dietrich, B.; Peter, G. J Cell Plast 1985, 21, 171.